Fullerene irradiation leading to track formation enclosing nitrogen bubbles in GaN material

JG Mattei, M. Sall, F. Moisy, A. Ribet, E. Balanzat, C. Grygiel, and I. Monnet*

CIMAP, CEA-CNRS-ENSICAEN-Normandie Université BP5133 F-14070 Caen cedex5 France.

* *Corresponding author:* monnet@ganil.fr

Abstract

Gallium nitride was irradiated with fullerene projectiles having an electronic stopping power above the threshold required to promote ion track formation. The structural and chemical changes induced by fullerene irradiation were studied through Transmission Electron Microscopy (TEM). High resolution TEM inquiries were performed to identify the structural order along the ion tracks and the strain induced in the lattice neighboring the ion tracks. The TEM investigation pointed out local amorphization inside the whole tracks and High Resolution TEM studies in the track periphery evidence local stress in the wurtzite structure. Chemical investigations were carried out by STEM - Electron Energy Loss Spectroscopy (EELS) to describe the chemical order in the neighboring and inside the ion path. Ga/N stoichiometry is essentially maintained in the track core, whereas an oxidation is detected in the ion track, at the surface. Furthermore, the nitrogen k near-edge fine structure investigation reveals the encapsulation of nitrogen bubbles inside the ion tracks.

KEYWORDS: *swift heavy ions, irradiation, GaN, nitrogen bubbles, transmission electron microscopy, electron energy loss spectroscopy, fine structure*

1. Introduction

Owing to their wide direct band gap, the nitride semiconductors, (Al,Ga,In)N can cover a large spectral range from the near infrared to ultraviolet, including the visible region. III-Nitrides exhibit remarkable optical and electronic properties promoting useful applications such as UV-photodetectors, laser diodes and light-emitting diode devices [1-5]. Among these nitride semiconductors, GaN demonstrates a high thermal stability making this material suitable for use in harsh environments. Therefore, such material is intended to become one of the next-generation technologies for space exploration [6,7], where radiation damage can strongly limit the efficiency of these future technologies. The devices will be subjected to particles such as protons, electrons, neutrinos, gamma rays and ions including swift heavy ions. For ions at low energy, the ion energy loss process is governed by nuclear collisions creating point defects and/or extended defects. For such energy, GaN does not behave as a classical semiconductor. In the case of most semiconductors, defects induced by low energetic ions are confined in the material approximately at the implantation distance/depth (projectile range Rp). In GaN, while defects accumulation also occurs in the projectile range region, an unusually strong surface damage, attributed to trapping of mobile point defects by the GaN surface, is observed. At high fluence, a highly disordered layer (100% of disorder in c-RBS) starts from the surface [8,9]. Some authors claimed that this highly disordered region is in fact nanocrystalline for GaN irradiated with rare earth at high fluences [10-12] or consists of randomly oriented nanocrystallites and N_2 bubbles embedded in an amorphous non-stoichiometric GaN matrix [13]. In any case, the maximum of damage is reached at the surface and not at the depth, near the implantation range, where most atomic displacements are induced. Furthermore, the chemical disorder induced by ion bombardment gives rise to N_2 bubbles formation in the outer layers [13-16].

On contrary, in the high energy range, electronic energy losses, Se, are predominant. It is well known that intense Se may lead to other kind of defects: latent track, phase transition and surface nanostructures. Ion track formation is governed by the electronic energy loss process according to various phenomenological models: Coulomb explosion, lattice relaxation and thermal spike [17-21]. High energetic ions, with Se above 17 keV/nm, usually produce tracks along the ion path in gallium nitride [22]. Undeniably, studies performed on this material have demonstrated that ion irradiation, at normal incidence with a high velocity, leads to discontinuous track formation [23]. In addition, an increase of the electronic stopping power induces latent tracks displaying more continuous morphology/shape [22]. Others studies found that swift heavy ion irradiation on GaN produces disordered tracks and generates lattice stress [24,25]. The impact produced by the projectile exhibits a circular area i.e. a track containing extended defects such as dislocations [22, 26]. In the surface region, other defects, such as nanoholes, were identified in the case of irradiation at grazing incidence [27]. Recently, A. Kumar et al. have reported that heavy ion irradiation induces the formation of isolated defect clusters which affect electrical properties [28-30]. Therefore, a better understanding of the loss of performance induced by irradiation requires investigating locally, at the atomic scale, the induced damage.

Transmission electron microscopy (TEM) has been extensively used to examine the effect of SHI on GaN material. In particular, latent tracks were widely investigated to recognize any structural modification. However, very few studies have assessed the chemical order in the ion track region. The main goal of this work is to develop a better understanding of atomic displacements and segregation which take place during and post irradiation. Electron energy loss spectroscopy (EELS) allows probing the chemical environment, typically at specific edges of gallium and nitrogen. This way, we are able to investigate locally the chemical order in the ion track region.

In a previous study, Sall et al. have reported a phase transition occurring along the ion path, resulting in some amorphization in the surface region [31]. Ions tracks were created using fullerene irradiation via

two projectiles C_{20} and C_{60}. Particularly, a full amorphization of the ion tracks originating from C_{60} were clearly established. However, the structural order inside ion tracks induced by C_{20} projectiles was not fully understood. Indeed, characterizations were, at this time, performed on a JEOL 2010 microscope and high-resolution investigation on ion tracks smaller than 1.6 nm suffered from dynamic and delocalization effects. This new study intends to describe more accurately the structural and the chemical order inside these ion tracks. To overcome obstacles of previous characterizations, a modern double Cs corrected transmission electron microscope fitted with EEL spectrometer has been used.

2. Experimental details

1. Materials and Methods:

The wurtzite GaN layers used in the current study are 3.5-µm-thick, epitaxially grown on c-plane sapphire substrates by metal organic chemical vapor phase deposition by St Gobain Crystals company (Vallauris, France), n-doped($1.9x10^{18}$ cm^{-3}).

Samples were pre-thinned prior to irradiation in a plan view configuration. They were prepared by a mechanical polishing up to a thickness of 100 µm, then dimpled down to a thickness of 10 µm at their centers and finished by by argon ion milling (5 keV) using a Gatan precision ion-polishing system. Irradiations were carried out at RT under normal incidence using 40 MeV C_{60} fullerene beams provided by the tandem accelerator at the Institut de Physique Nucléaire d'Orsay, IPNO, (Orsay, France). The 40 MeV C_{60} ion beam was, to a certain degree, contaminated by12 MeV C_{20}.Irradiation on thin sample allows analyzing a region where carbon cluster integrity is conserved, and can still be considered as a single projectile. The implantation region of the ions is avoided and the slowing down regime is predominately ruled by electronic processes.

For each irradiation, Table I displays the corresponding S_e, the energy deposited by electronic excitation for a given fluence.

Projectile	**Energy (MeV)**	**Se ($keV.nm^{-1}$)**	**Fluence ($ions.cm^{-2}$)**
C_{60}	40	59	10^{11}
C_{20}	12	19	10^{11}

Table 1 - Irradiation parameters for C_{60} and C_{20} projectiles in GaN. Se value corresponds to the value at the entrance in the target

2. Characterization techniques:

High resolution TEM and STEM experiments were performed on a double corrected JEOL ARM 200F operating at 200 kV fitted with a GIF Quantum Gatan energy filter. In STEM mode, this microscope provides a spatial resolution of 0.078 nm. STEM analyses were carried out using an HAADF detector at inner and outer angles of 68 and 280 mrad to efficiently reduce diffraction contrasts. EELS experiments were performed with a collection angle of 90 mrad. Elemental mapping were recorded with a dispersion of 1eV/channel while ELNES spectra were acquired using an energy dispersion of 0.025eV/channel providing an energy resolution of 0.5 eV. HR-TEM/STEM micrographs and EELS data were acquired and processed under Gatan Digital Micrograph environment.

3. Results/discussion

We investigated a gallium nitride sample irradiated with fullerenes. As mentioned previously in the experimental details, the sample was thinned prior to irradiation, thus this study is not representative of a bulk material response but rather representative of a near surface region response. For this study, two kinds of projectiles were used: 40 MeV C_{60} and 12 MeV C_{20} which provide respectively Se value of 59 and 19 keV/nm (table 1). Such electronic stopping powers are sufficient to overcome the Se threshold (17 keV/nm) in gallium nitride promoting ion track formation.

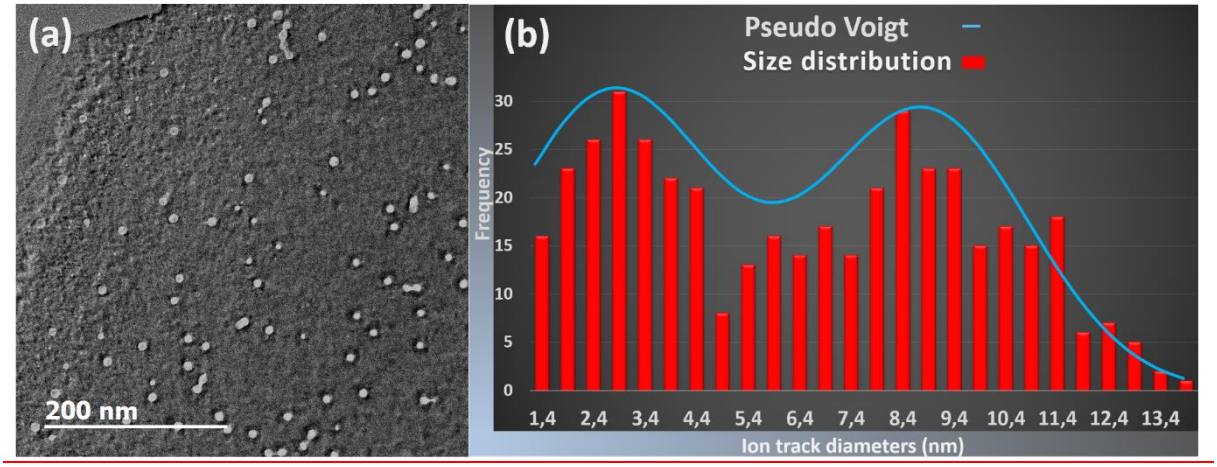

Fig.1. a) TEM plan view micrograph of GaN irradiated, b) Size distribution of ion track diameters.

TEM investigations reveal different latent tracks induced by fullerene projectiles. The TEM micrograph of a GaN specimen plan view, displayed in Fig. 1a, shows several tracks diameters. Most of the tracks are isolated but we can sometimes observe some overlapping tracks. A size distribution was performed on 427 ion tracks to obtain better statistics. Measurement of small track diameters was performed on high resolution TEM images. Although this method could appear to be tedious work, it was necessary to measure track diameters of about 1-2 nm. This way, the track diameter is measured from the last atomic layer surrounding the amorphous track. Size distribution (Fig. 1b) reveals two kinds of populations. A first ion track population, assigned to C_{20} projectiles, displays a mean diameter of 2.8 nm. The second population, originating from C_{60} projectiles, exhibits a higher mean diameter of 8.5 nm. Latent tracks observed on Fig. 1 display a brighter contrast compared to their surrounding region, this could be attributed to the loss of matter in the track region and/or to structural modification. Thus, high resolution TEM investigations were carried out to describe the structural order within ion track region.

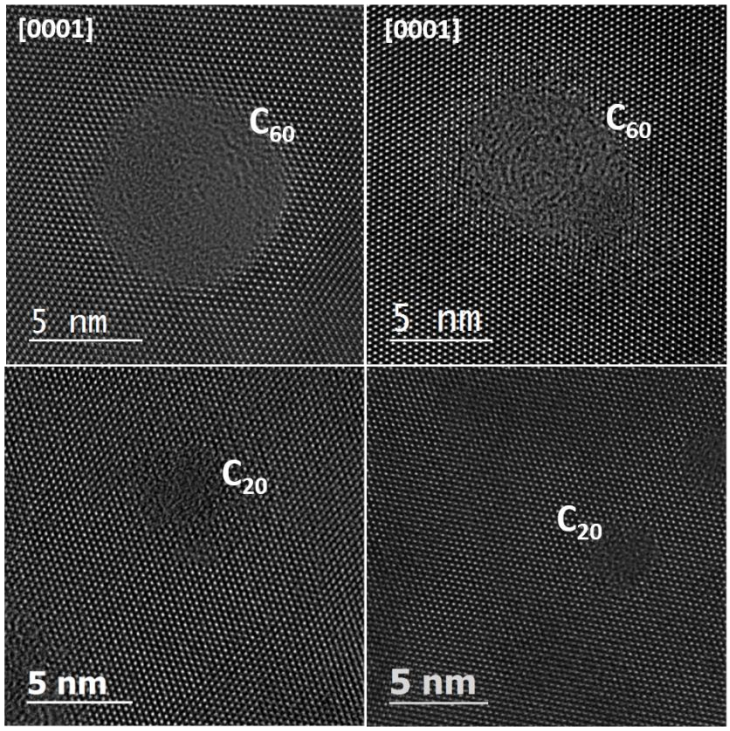

Fig.2. High-Resolution TEM micrographs of amorphous ion tracks. Plan views of wurtzite GaN are oriented along the [0001] zone axis.

These High resolution TEM analyses were performed along the [0001] zone axis of the wurtzite structure. TEM images (Fig. 2) exhibit two kinds of track diameters: larger tracks correspond to C_{60} projectiles while smaller tracks are assigned to C_{20} projectiles. This is a new result compared with the last study which clearly establishes irradiation with C_{20} leads to amorphous track as well [31]. It should be noted that during TEM investigations, electron beam could induce a partial recrystallization of the ion tracks.

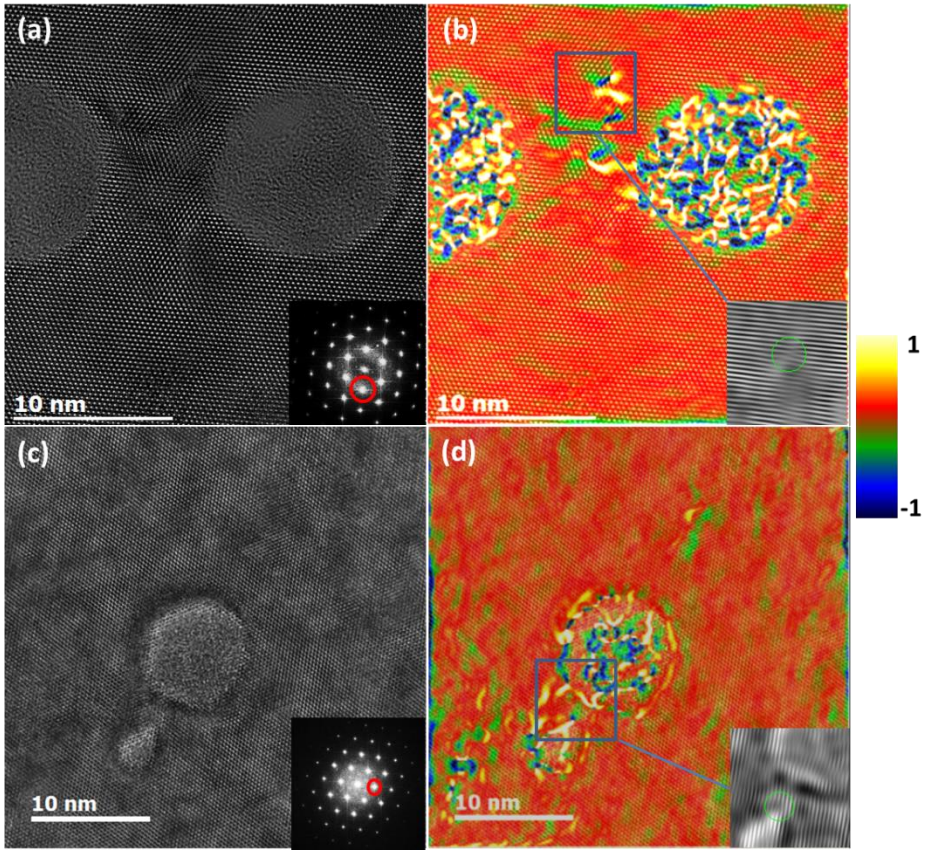

Fig.3.a) HRTEM image of GaN plan view along the [0001] zone axis, the FFT is displayed in an inset, b) micrograph superimposed to the strain map of $(0\bar{1}10)$ reflexion measured by geometrical phase analysis (zoom of a dislocation is shown in the inset), c) HRTEM micrograph of C_{60} and C_{20} projectile and its respective, d) GPA strain map of $(10\bar{1}0)$ (zoom of dislocation is shown in inset).

In addition, the investigation of the structural order on the track borders reveals some defects induced by ion bombardments. This stress seems occurring along the $(0\bar{1}10)$ planes. Fig. 3a shows a high resolution TEM micrograph oriented along the [0001] zone axis of the wurtzite structure. On this picture, two ion tracks, originating from two C_{60} projectiles, are observed. Between these tracks, clear defects are identified. To illustrate this result, Geometric Phase Analysis was performed to map the displacement of the planes associated to the $(0\bar{1}10)$ reflexion. The colored map superimposed to the HRTEM micrographs shows the variation ($\delta[0\bar{1}10]$) of the lattice plane spacing (Fig. 3b,d). Thus, this displacement map reveals clear defects between tracks such as dislocations (Fig.3b). Some stress was recognized on the track border as well. Fig. 3c displays a TEM micrograph in which we observe two ions tracks. The small one is related to a C_{20} projectile on contrary to larger track generated by a C_{60} projectile. An extended defect is evidenced between these two tracks. The strain mapping (deriving from GPA analysis) focused on this reflection confirms the presence of such defect (Fig. 3d) which can be assigned to a stacking fault or a misfit dislocation. Furthermore, this strain map reveals some strain localized around the ion track periphery of C_{60} projectiles. This strain is not exactly localized on the track border but about 1.5 nm around the ion track. It could be related to a defect induced by the ion track or linked to nanohillock formation in surface, resulting in a surface thickness alteration surrounding the ion track.

Furthermore, we carried out scanning transmission electron microscopy in high-angle annular dark-field (HAADF) mode to check the intensity in the ion track periphery. Fig. 4a shows a STEM HAADF image containing several ion tracks. On the track border, an increase of the intensity is clearly observed if we compare to the bulk intensity (Fig. 4b). As HAADF intensity is proportional to the square of the atomic number, $I_{haadf} \sim t.Z^2$. This result could be related to a higher concentration of both gallium and nitrogen. However, t parameter is assigned as the thickness of the sample. Thus, this higher intensity could also be linked to an increase of the thickness surrounding the ion track. Moreover, it has been also reported that higher HAADF intensity could be related to strain field as well [32]. To answer these questions, we examined first the thickness variation of ion tracks region using energy filtered TEM (EFTEM) imaging.

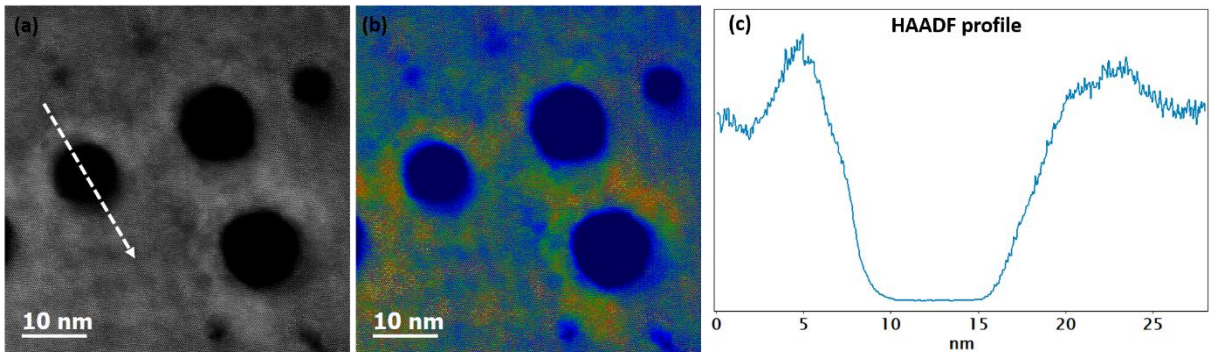

Fig.4. a) A plan view HAADF image of GaN exhibiting latent tracks, b) the corresponding HAADF image using a temperature CLUT (color lookup table), c) HAADF intensity profile of a latent track.

The thickness of the ion track region was measured using the log-ratio method. Fig. 5a. displays the relative thickness map (thickness/mean free path) of an ion track region acquired using the EFTEM mode. Fig. 5b presents the same thickness map but displayed as a 3D plot to emphasize the thickness variation. Thus, we can first observe some small tracks (indicated by blue arrows in inset) probably induced by C_{20} projectiles which appears hollow in term of thickness variation. Interestingly, the larger tracks, related to C_{60} projectiles, display in fact a crater shape. However, it is well known that strongly diffracting zones might induce some artefacts in EFTEM images. As seen in Fig. 3, some strain field has been evidenced in the ion track periphery and could thus induce these artefacts in EFTEM images. Nevertheless, some AFM measurements (not shown here) seem to be in line with these crater shapes. Further investigations will be conducted in the future to describe more accurately these specific shapes.

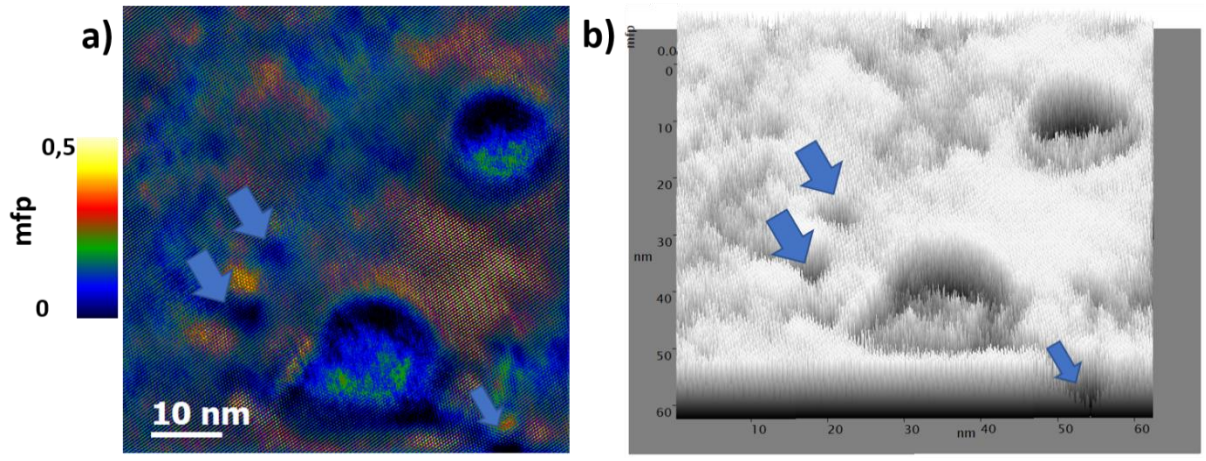

Fig.5. a) Relative thickness map using EFTEM mode, the color is based on the t/λ scale (mean free path), b) relative thickness map displayed as a 3D surface plot

Subsequently, we investigated the chemical order in the neighbourhood of an ion track to identify any change in the nitrogen or gallium track content. Thus, EELS analyses were carried out at different ionization edges: nitrogen K edge and gallium $L_{2,3}$ edge. Furthermore, this technique is quite sensitive to light elements such as carbon or oxygen, for that reason we focused as well on the oxygen K edge. Hence, we performed an EELS mapping on a specific ion track induced by C_{60} (Fig.6a). EELS mapping at gallium and nitrogen edges confirms a decrease, into the track of their respective ratio to the bulk concentration. The relative decrease of Ga and N is basically the same, indicating that stoichiometry is preserved. Besides, oxygen K edge were also observed on EELS spectra and localized exactly on the track periphery. This result is even more enhanced on the EELS profile, originated from EELS mapping and plotted along a line crossing the whole ion track diameter (Fig.6b). As such, we observe a clear enhancement of the oxygen ratio on the track border. It is perhaps appropriate to remind here that STEM analyses are 2D projections. Hence, we cannot affirm if oxidation occurs on the surface or inside the material. Besides, irradiations were performed at normal incidence, directly on a GaN plan view TEM sample, and SHI are well known to induce nano hillocks or crater at the surface (as observed on Fig. 5). It is most likely that oxygen is ab/adsorbed in the periphery of the ion tracks as we did not find any TEM evidence of the formation of known oxides phases.

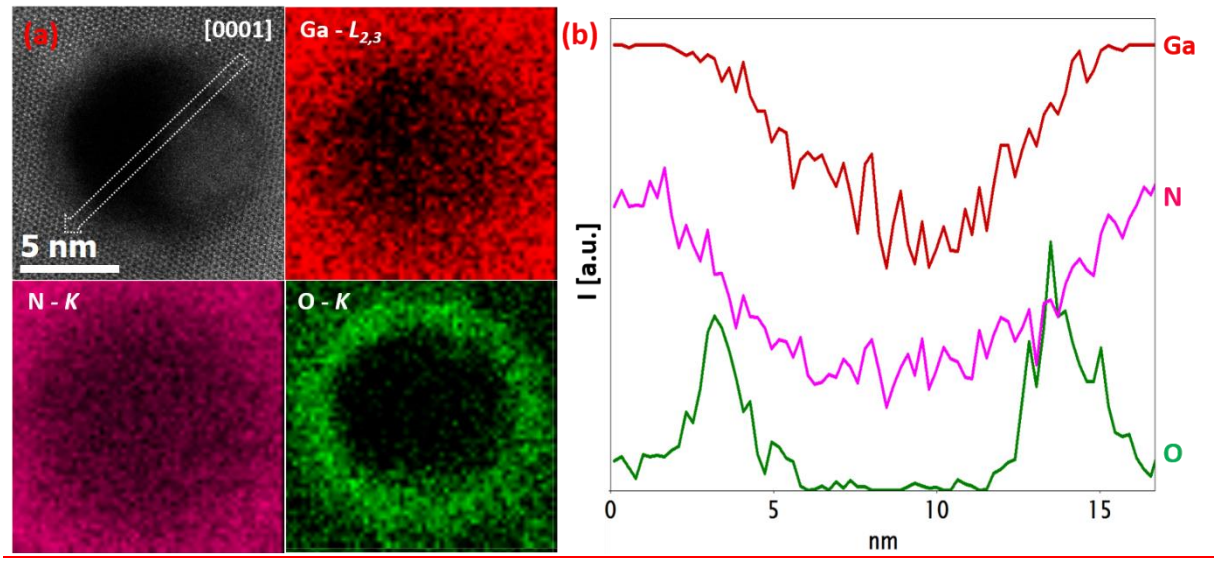

Fig.6.a) ADF image and EELS mapping of gallium $L_{2,3}$ edge (red), nitrogen K edge (purple) and oxygen K edge (green), b) EELS profile of Ga, N and O accross ion track

To go further and describe the local atomic environment in the track region, we investigated the Energy Loss Near Edge Structure (ELNES) at nitrogen K edge. Indeed, many studies have been performed at nitrogen edge for this kind of material. Nitrogen K edge fine structure is useful to distinguish the hexagonal and the cubic phase in gallium nitride for instance. Thus, fine structure studies were first performed using point EELS analysis in three different regions: bulk region, track border and the track core region (Fig.7a). Fig.7b shows the different ELNES spectra acquired in these three regions. Nitrogen K edge fine structure in the bulk region (spectrum 1) displays a specific shape of the hexagonal wurtzite gallium nitride (h-GaN) [33], however EELS analysis in the track border shows a pre-peak (ELNES

spectrum 2), finally nitrogen K edge fine structure inside the ion track shows a thinner peak at 398 eV (ELNES spectrum3).

Two dashed arrows are displayed to illustrate peaks of the near edge fine structure (A and B). From our experimental data ΔAB is about 2.4 eV which is consistent with Lazar observation for h-GaN [33]. Moreover, we clearly observe an enhancement of A-peak intensity related to the track border region. Katsikini et al. have observed this kind of fine structure using XANES investigations [34]. According to the literature, point defects usually lead to empty states in the midgap depending on different configurations: nitrogen interstitial, substitution of Ga with N atom (N_{Ga}) and substitution of N with Ga atoms (Ga_N). They first excluded substitution of N atom with Ga; consequently, such atomic arrangement would lead to Ga-Ga bonds which could not be identified at nitrogen K edge. Nitrogen interstitial signature is supposed to be localized 1.7 eV below the N *K* edge which is not clearly observed on Fig.7. According to their study, A-peak could be related to nitrogen dangling bonds which means that gallium atom is thus missing. Finally, A-peak could be assigned as a gallium vacancy; moreover, this result is also supported by the work of Xin [35]. Their study at Nitrogen *K edge* ELNES performed by EELS analyses evidence a pre edge similar to A-peak. This peak was identified on a pure edge dislocation with a Ga vacancy.

However, the nitrogen K edge ELNES 3 displays a thinner single-peak with a higher intensity which is quite different from that of the h-GaN fine structure. Indeed, many studies have reported such fine structure for nitrogen gas; Lacroix et al. evidenced molecular N_2 inside nanopores in a SiO_xN_y matrix. The ELNES spectrum of N_2 fine structure reported in this paper is clearly comparable to our result [36]. Kovacs et al. identified a similar fine structure by recording EELS spectrum in TEM under molecular gas N_2 environment [37]. These experiments were performed to prove the inclusion of N_2 molecules in a GaN matrix. Indeed, the nitrogen K edge ELNES observed on the spectrum 3 is the specific signature of N_2 molecule. Thus, this result evidences the presence of dinitrogen gas inside the ion track. Furthermore, we should remind this TEM plan view was prepared by ion milling with 5keV Ar^+ and then exposed to fullerene bombardment. Thus, low energetic ions which could be provided by Focus Ion Beam and thus inducing point defect were avoided. Therefore, dinitrogen gas formation is clearly related to C_{60} impacts.

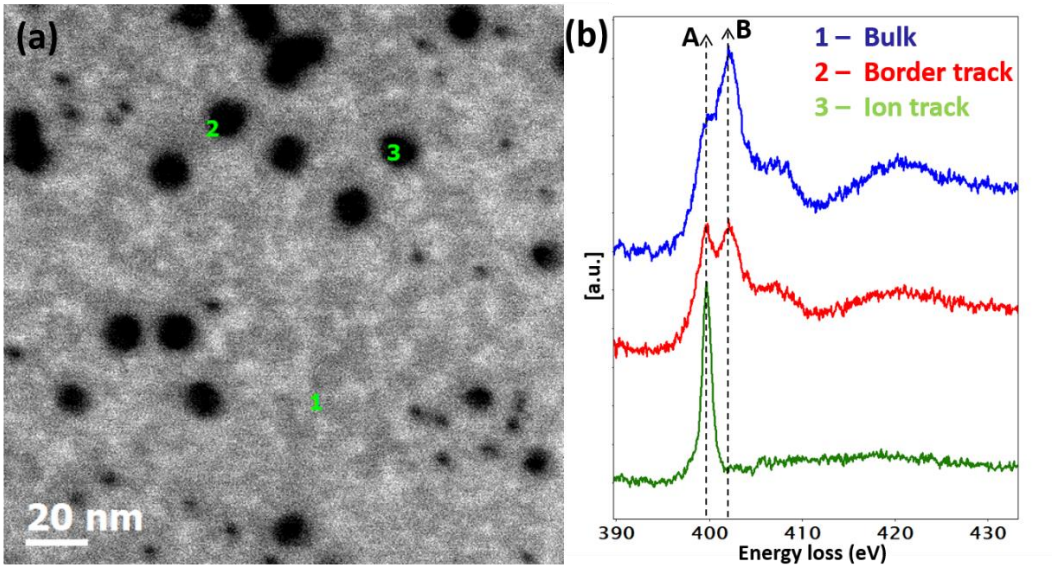

Fig.7. a) A plan view HAADF image of GaN and latent tracks b) Nitrogen K – ELNES spectra in several regions: 1-bulk region in blue line, 2-track border (spectrum plotted in red), 3- ion track core (green spectrum).

Concerning the ELNES observed on the track border (spectrum 2 - red spectrum), another explanation would be that enhancement of A-peak is explained by a superposition of N_2 and h-GaN fine structure [37]. However, we observed such overlapping in our experiment; A-peak appears to be more intense than B peak related to h-GaN. Therefore, A peak in the ELNES spectrum 2 could be likely attributed to Ga vacancy, in agreement with the study of Xin et al. [35].

To go further we performed EELS mapping on several tracks in order to increase the statistic. EELS spectra were acquired with an energy dispersion of 0.025eV/channel in order to map the nitrogen K edge fine structure (Fig.8). Defining the spatial distribution of chemical states requires distinguishing h-GaN fine structure from N_2 fine structure. Thus, we performed, using digital micrograph software, Multiple Linear Least Squares (MLLS) fitting according to two near edge fine structures references: N_2 gas and h-GaN. MLLS fitting enables to differentiate these two environments and to fit these specific fine structures in the spectrum image.

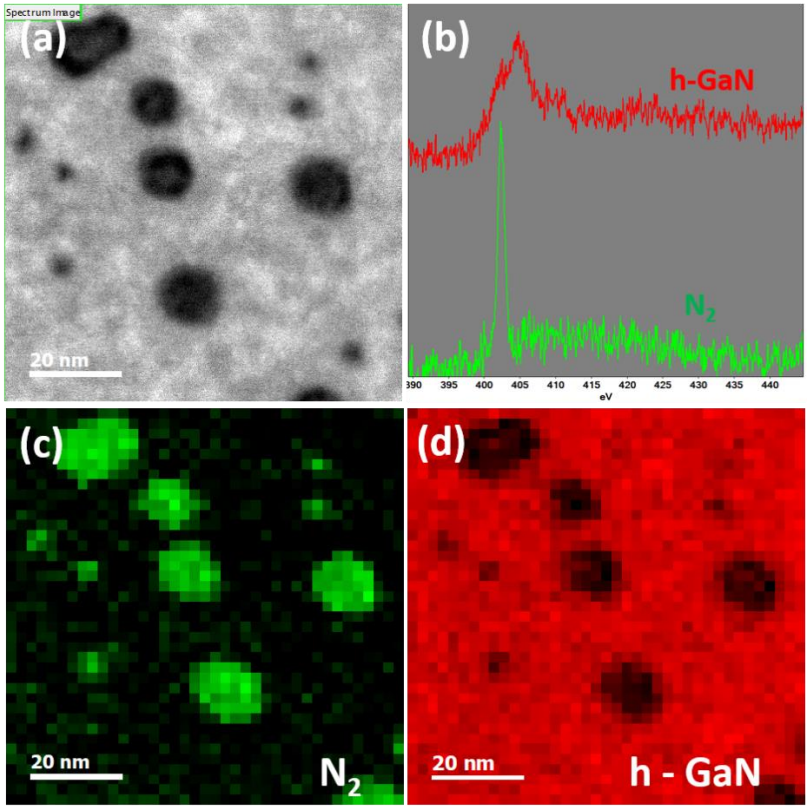

Fig.8a) STEM HAADF image b) h-GaN and N_2 reference spectra c) Nitrogen K near-edge structure mapping for N_2 (green) d) ELNES for h-GaN (red)

Fig.8a shows the ADF image probed for EELS analysis, the two ELNES references for N_2 molecule and for the hexagonal GaN (h-GaN) (Fig.7b) and the respective ELNES mapping (Figs.8 c and d). Thus, ELNES mapping revealing h-GaN is mainly localized in the bulk part as expected. ELNES h-GaN intensity is quite low in the track region due to the amorphization of GaN. On the contrary, nitrogen fine structure specific of nitrogen gas is observed inside each ion track. Thus, this result clearly evidences that N_2 gas is trapped within every ion track. Thus, dinitrogen gas formation is clearly related to C_{60} and to C_{20} impacts as well.

Several previous studies have also reported the formation of nitrogen bubbles in a GaN matrix submitted to irradiation. However, these irradiations were performed in the nuclear energy loss range (1 or 2 MeV Au+), which induces point defects, leading to amorphization of GaN in surface. Kucheyev et al. reported that N_2 formation induces a high nitrogen loss in GaN matrix [9]. In our case, fullerene irradiation produces, locally, an intense electronic excitation which induces a confined enhancement of the temperature. According to gallium nitride phase diagram, a temperature beyond 1117 K decomposes GaN into pure gallium liquid and nitrogen gas [38,39]. Consequently, as nitrogen gas was identified in this ion track, this suggests a pure gallium formation as well, which would be consistent with the in-track conservation of the bulk Ga/N stoichiometry observed in Fig. 5b.

Nevertheless, it should be noted that some authors identified N_2 bubbles formations in an amorphous layer of GaN induced by irradiation at lower energy (4.7 MeV Au), however no Ga-Ga bonding were identified. Indeed, they observed a great decrease of Ga coordination number [13]. Other reports pointed out that, in addition to the N-N bonds, Ga-Ga bonds were created as well by phase segregation during

irradiation and that nitrogen bubbles induce, locally, high pressure on the lattice [14,40,41]. Apart from the controversy about Ga-Ga bonds, this observation is consistent with the extended defects identified in the ion track periphery in our high resolution TEM investigations. Accordingly, the stress identified on the track region could be related to a high-pressure induced by nitrogen bubbles. Since N_2 gas is clearly identified in the ion track region, nitrogen bubbles must be encapsulated in. Moreover, Ga vacancies are observed through EELS investigations in the track periphery. All this goes to show that a GaN dissociation probably occurred. Therefore, we can reasonably assume that tracks contain N_2 gas enclosed in an amorphous Ga or GaN matrix.

4. Conclusion

Gallium nitride was irradiated with C_{20} and C_{60} clusters using a Se value above the electronic stopping power threshold for ion track formation. Despite the cluster size, both projectiles lead to phase transition. TEM investigation pointed out local amorphization inside the whole tracks. High Resolution TEM studies in the track periphery evidence a local stress in the wurtzite structure. EELS analyses have demonstrated chemical environment changes such as oxidation in the track border, while a reduction of nitrogen and gallium content was identified inside the tracks. The analysis of nitrogen K edge fine structure reveals a fine structure typical of gallium vacancy in the track periphery while a clear signature of dinitrogen gas fine structure is observed inside the track. This specific signature of N_2 is identified in each ion track, which gives evidence of encapsulation of nitrogen bubbles inside the ion tracks. To the best of our knowledge, this is the first-time nitrogen gas or nitrogen dimmer is observed specifically inside ion tracks produced by SHI.

Acknowledgements

The authors would like to thank the ALTO accelerators team for providing the ion beams. M. Sall. is grateful to the “Région Basse-Normandie” for its partial contribution to his doctoral grant. This work was partially supported by the ANR funding “Investissements d’avenir” ANR-11-EQPX-0020 (Equipex GENESIS) and ANR-10-LABX-09-01 (LabEx EMC3), by the “Fonds Européen de Developpement Regional” and by the Region Basse-Normandie.

Additional Information

Competing Interests: The authors declare no competing interests.

References

[1] F. Ponce, D. Bour, Nitride-based semiconductors for blue and green light-emitting devices, Nature. 386 (1997) 351-359.

[2] Y. Huang, X. Duan, Y. Cui, and C.M. Lieber, Gallium nitride nanowire nanodevices. Nano Letters, 2(2) (2002): 101-104.

[3] S. Nakamura, S. Pearton, & Fasol, G. The blue laser diode: the complete story, Measurement Science And Technology. 12 (2001) 755-756.

[4] S. Nakamura, M. Senoh, N. Iwasa, S. Nagahama, T. Yamada, T. Mukai, Superbright Green InGaN Single-Quantum-Well-Structure Light-Emitting Diodes, Japanese Journal Of Applied Physics. 34 (1995) L1332-L1335.

[5] A. Khan, K. Balakrishnan, &T. Katona, Ultraviolet light-emitting diodes based on group three nitrides. Nature photonics, 2(2), (2008) 77.

[6] J. Ackermann, N. Angert, R. Neumann, C. Trautmann, M. Dischner, T. Hagen, M.Sedlacek, Ion track diameters in mica studied with scanning force microscopy, Nuclear Instruments And Methods In Physics Research Section B: Beam Interactions With Materials And Atoms. 107 (1996) 181-184.

[7] S. Mansouri, P. Marie, C. Dufour, G. Nouet, I. Monnet, H. Lebius, Swift heavy ions effects in III–V nitrides, Nuclear Instruments And Methods In Physics Research Section B: Beam Interactions With Materials And Atoms. 266 (2008) 2814-2818.

[8] S. Kucheyev, J. Williams, C. Jagadish, J. Zou, G. Li, Damage buildup in GaN under ion bombardment, Physical Review B. 62 (2000) 7510-7522.

[9] S. Kucheyev, J. Williams, C. Jagadish, J. Zou, V. Craig, G. Li, Ion-beam-induced porosity of GaN, Applied Physics Letters. 77 (2000) 1455-1457.

[10] K. Lorenz, N. Barradas, E. Alves, I. Roqan, E. Nogales, R. Martin,K. P. O'Donnell, F. Gloux and P. Ruterana, Structural and optical characterization of Eu-implanted GaN, Journal Of Physics D: Applied Physics. 42 (2009) 165103.

[11] F. Gloux, T. Wojtowicz, P. Ruterana, K. Lorenz, E. Alves, Transmission electron microscopy investigation of the structural damage formed in GaN by medium range energy rare earth ion implantation, Journal Of Applied Physics. 100 (2006) 073520.

[12] P. Ruterana, B. Lacroix, K. Lorenz, A mechanism for damage formation in GaN during rare earth ion implantation at medium range energy and room temperature, Journal Of Applied Physics.

[13] M. Ridgway, S. Everett, C. Glover, S. Kluth, P. Kluth, B. Johannessen,Z.S.Hussain, D.J.Llewellyn, G.J.Foran, G. de M.Azevedo, Atomic-scale structure of irradiated GaN compared to amorphised GaP and GaAs, Nuclear Instruments And Methods In Physics Research Section B: Beam Interactions With Materials And Atoms. 250 (2006) 287-290.

[14] M. Ishimaru, Y. Zhang, W. Weber, Ion-beam-induced chemical disorder in GaN, Journal Of Applied Physics. 106 (2009) 053513.

[15] S. Kucheyev, J. Williams, J. Zou, C. Jagadish, G. Li, Ion-beam-induced dissociation and bubble formation in GaN, Applied Physics Letters. 77 (2000) 3577-3579.

[16] W. Jiang, Y. Zhang, W. Weber, J. Lian, R. Ewing, Direct evidence of N aggregation and diffusion in Au+ irradiated GaN, Applied Physics Letters. 89 (2006) 021903.

[17] A. Dunlop, D. Lesueur, P. Legrand, H. Dammak, J. Dural, Effects induced by high electronic excitations in pure metals: A detailed study in iron, Nuclear Instruments And Methods In Physics Research Section B: Beam Interactions With Materials And Atoms. 90 (1994) 330-338.

[18] P. Stampfli, Electronic excitation and structural stability of solids, Nuclear Instruments And Methods In Physics Research Section B: Beam Interactions With Materials And Atoms. 107 (1996) 138-145.

[19] P. Stampfli, K. Bennemann, Theory for the instability of the diamond structure of Si, Ge, and C induced by a dense electron-hole plasma, Physical Review B. 42 (1990) 7163-7173.

[20] M. Toulemonde, W. Assmann, C. Dufour, A. Meftah, C. Trautmann, Nanometric transformation of the matter by short and intense electronic excitation: Experimental data versus inelastic thermal spike model, Nuclear Instruments And Methods In Physics Research Section B: Beam Interactions With Materials And Atoms. 277 (2012) 28-39.

[21] M. Toulemonde, E. Paumier, C. Dufour, Thermal spike model in the electronic stopping power regime, Radiation Effects And Defects In Solids. 126 (1993) 201-206.

[22] F. Moisy, M. Sall, C. Grygiel, A. Ribet, E. Balanzat, I. Monnet, Optical bandgap and stress variations induced by the formation of latent tracks in GaN under swift heavy ion irradiation, Nuclear Instruments And Methods In Physics Research Section B: Beam Interactions With Materials And Atoms. 431 (2018) 12-18.
[23] S. Kucheyev, H. Timmers, J. Zou, J. Williams, C. Jagadish, G. Li, Lattice damage produced in GaN by swift heavy ions, Journal Of Applied Physics. 95 (2004) 5360-5365.
[24] F. Moisy, M. Sall, C. Grygiel, E. Balanzat, M. Boisserie, B. Lacroix,P.Simon, I.Monnet, Effects of electronic and nuclear stopping power on disorder induced in GaN under swift heavy ion irradiation, Nuclear Instruments And Methods In Physics Research Section B: Beam Interactions With Materials And Atoms. 381 (2016) 39-44.
[25] P. Hu, J. Liu, S. Zhang, K. Maaz, J. Zeng, H. Guo,P.F. Zhai,J.L. Duan, Y.M. Sun, M.D. Hou, Raman investigation of lattice defects and stress induced in InP and GaN films by swift heavy ion irradiation, Nuclear Instruments And Methods In Physics Research Section B: Beam Interactions With Materials And Atoms. 372 (2016) 29-37.
[26] S. Mansouri, P. Marie, C. Dufour, G. Nouet, I. Monnet, H. Lebius, Swift heavy ions effects in III–V nitrides, Nuclear Instruments And Methods In Physics Research Section B: Beam Interactions With Materials And Atoms. 266 (2008) 2814-2818.
[27] M. Karlušić, R. Kozubek, H. Lebius, B. Ban-d'Etat, R. Wilhelm, M. Buljan,Z. Siketić, F. Scholz, T. Meisch, M. Jakšić, Response of GaN to energetic ion irradiation: conditions for ion track formation, Journal Of Physics D: Applied Physics. 48 (2015) 325304.
[28] A. Kumar, R. Singh, P. Kumar, U. Singh, K. Asokan, P. Karaseov A. I. Titov,D. Kanjilal, In-situ transport and microstructural evolution in GaN Schottky diodes and epilayers exposed to swift heavy ion irradiation, Journal Of Applied Physics. 123 (2018) 161539.
[29] A. Kumar, A. Hähnel, D. Kanjilal, R. Singh, Electrical and microstructural analyses of 200 MeV Ag14+ion irradiated Ni/GaN Schottky barrier diode, Applied Physics Letters. 101 (2012) 153508.
[30] A. Kumar, T. Kumar, A. Hähnel, D. Kanjilal, R. Singh, Dynamics of modification of Ni/n-GaN Schottky barrier diodes irradiated at low temperature by 200 MeV Ag14+ ions, Applied Physics Letters. 104 (2014) 033507.
[31] M. Sall, I. Monnet, F. Moisy, C. Grygiel, S. Jublot-Leclerc, S. Della–Negra, M Toulemonde, E. Balanzat, Track formation in III-N semiconductors irradiated by swift heavy ions and fullerene and re-evaluation of the inelastic thermal spike model, Journal Of Materials Science. 50 (2015) 5214-5227.
[32] L. Marks, P. Voyles, When is Z-Contrast D-Contrast?, Microscopy Today. 22 (2014) 65-65.
[33] [11] S. Lazar, G. Botton, M. Wu, F. Tichelaar, H. Zandbergen, Materials science applications of HREELS in near edge structure analysis and low-energy loss spectroscopy, Ultramicroscopy. 96 (2003) 535-546.
[34] M. Katsikini, F. Pinakidou, E. Paloura, W. Wesch, Identification of implantation-induced defects in GaN: A near-edge x-ray absorption fine structure study, Applied Physics Letters. 82 (2003) 1556-1558.
[35] Y. Xin, E. James, I. Arslan, S. Sivananthan, N. Browning, S. Pennycook,F. Omnès, B. Beaumont, J-P. Faurie, P. Gibart, Direct experimental observation of the local electronic structure at threading dislocations in metalorganic vapor phase epitaxy grown wurtzite GaN thin films, Applied Physics Letters. 76 (2000) 466-468.
[36] B. Lacroix, V. Godinho, A. Fernández, Nitrogen Nanobubbles in a-SiOxNy Coatings: Evaluation of Its Physical Properties and Chemical Bonding State by Spatially Resolved Electron Energy-Loss Spectroscopy, The Journal Of Physical Chemistry C. 120 (2016) 5651-5658.
[37] A. Kovács, B. Schaffer, M. Moreno, J. Jinschek, A. Craven, T. Dietl,A. Bonanni, R. E. Dunin-Borkowski, Characterization of Fe-N nanocrystals and nitrogen–containing inclusions in (Ga,Fe)N thin films using transmission electron microscopy, Journal Of Applied Physics. 114 (2013) 033530.
[38] W. Utsumi, H. Saitoh, H. Kaneko, T. Watanuki, K. Aoki, O. Shimomura, Congruent melting of gallium nitride at 6 GPa and its application to single-crystal growth, Nature Materials. 2 (2003) 735-738.
[39] R. E. D. Rivas, Growth of GaN Nanowires: A Study Using In Situ Transmission Electron Microscopy (Doctoral dissertation, Arizona State University). (2010)
[40] I. Bae, W. Jiang, C. Wang, W. Weber, Y. Zhang, Thermal evolution of microstructure in ion-irradiated GaN, Journal Of Applied Physics. 105 (2009) 083514.
[41] W. Jiang, Y. Zhang, W. Weber, J. Lian, R. Ewing, Direct evidence of N aggregation and diffusion in Au+ irradiated GaN, Applied Physics Letters. 89 (2006) 021903.